

Solar Flare Observations with the RNO-G detector

M. Mikhailova,^a S. Hallman,^{a,b} D.Besson^{a,*} and the RNO-G Collaboration

^a*KU Physics Dept, Lawrence, KS USA*

^b*Deutsches Elektronen-Synchrotron DESY, Platanenallee 6, 15738 Zeuthen, Germany*

E-mail: m.mikhailova@icecube.wisc.edu, steffen.hallman@desy.de

Although designed for detection of cosmic ray neutrinos, the RNO-G detector serendipitously registered signals on Sept. 29, 2022 (approximately 48 hours before illumination of the solar panels fell below threshold to power the array) which were ultimately traced to a solar flare event on that day. Closer examination of the 2022 and 2023 RNO-G data revealed almost 100 solar flare events, each of which produced anywhere from tens to hundreds of triggers in the RNO-G stations. We detail, in this contribution, how those events were identified and subsequently used to calibrate the positions of the in-ice antennas on centimeter scales.

Acoustic and Radio EeV Neutrino Detection Activities (ARENA24), June 11–14, 2024, Chicago, IL USA

*Speaker

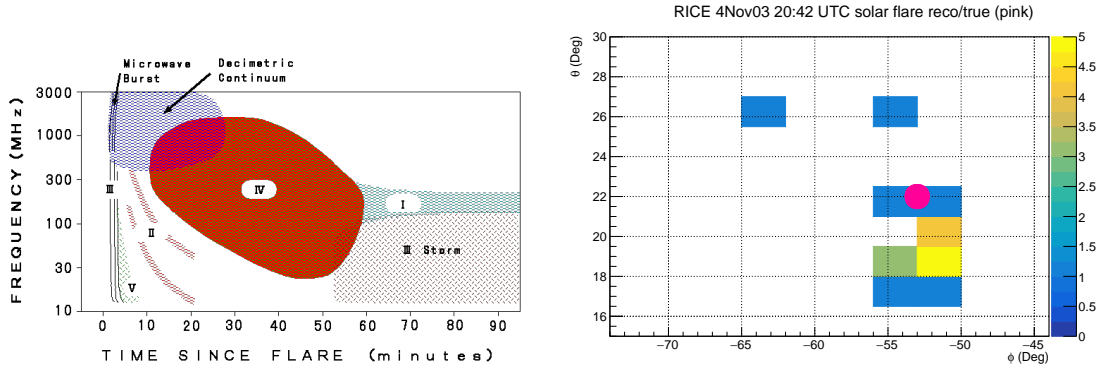


Figure 1: Left: Taxonomy of solar flares, classified by spectral content and duration. Flares discussed herein are predominantly Type III. Figure taken from <https://research.njit.edu/cstr/>. Right: RICE Solar reconstruction of 4Nov23 flare in azimuth vs. elevation; red circle indicates true location of sun (after correcting for refraction) at the time these data were taken.

"I believe the first draft of [conference proceedings] should take no more than three months. Any longer and the story begins to take on an odd foreign feel, like a dispatch from the Romanian Department of Public Affairs, or something broadcast on shortwave radio during a period of severe sunspot activity."

-Stephen Z. King, 2000

1. Solar Flare Observations in UHEN experiments

Since the first observation of solar flares in 1859 by Carrington and Hodgson[2], and the subsequent Earth-wide auroral activity that event engendered (the so-called ‘Carrington event’), solar flares have been the subject of concerted scientific study, in their own right, as well as a source of anxiety for the worldwide energy grid. Synchronized to sunspot activity, flaring activity on the sun also follows the same 11-year cycle observed for sunspots.

In addition to optical emissions, solar flares are also capable of generating significant radio-frequency (RF) power as magnetic field lines detach and reconnect on, and above the solar surface, resulting in rapid acceleration and deceleration of plasma. These RF emissions offer an infinite-distance calibration source for neutrino detectors based on RF technology, allowing cross-calibration of multiple receivers illuminated by a uniform plane wave. The RNO-G experiment[1] includes both under-ice and above-ice antennas, both with sensitivity to solar emissions.

Over the frequency band relevant to the RNO-G experiment, solar flares are broadly classified into 5 separate categories, distinguished by their duration and spectral power (Figure 1).

The first radio-frequency ultra-high energy neutrino detector (RICE, at the South Pole) noticed enhanced above surface RF emissions at an azimuthal angle inconsistent with the bulk of surface-generated background noise[3]. That event produced 18 reconstructable triggers over a 3 minute period (effectively saturating the RICE data-taking bandwidth), yielding the crude reconstruction shown. In addition to observation of solar flares in February, 2011 during the last solar cycle by the

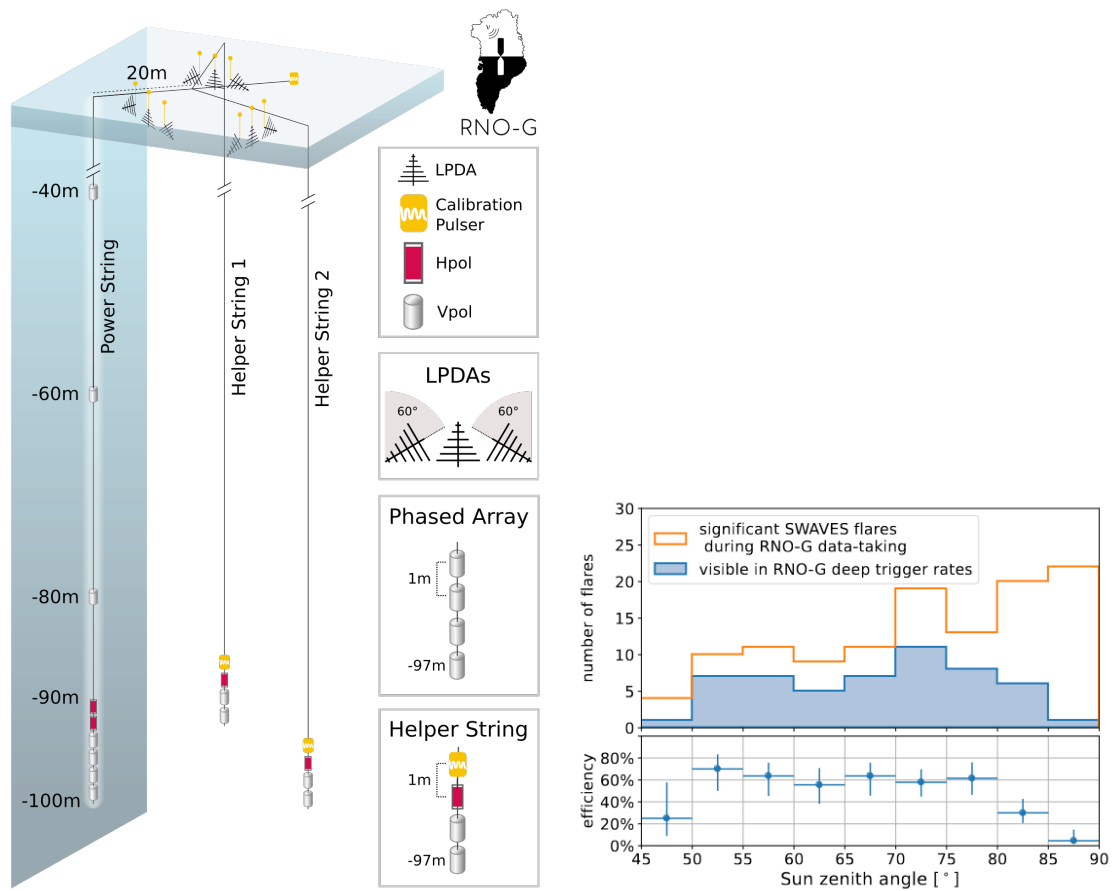


Figure 2: Left: Layout of RNO-G station receivers. Solar flares discussed herein are exclusively triggered in the deep ‘Phased Array’ antenna receiver channels, which require that two of the four VPol antenna channels exceed a pre-defined threshold, constituting a slightly less restrictive criterion than for the above-surface channels. Right: Summary of RNO-G solar flare trigger efficiency. Orange histogram shows flares identified by SWAVES observatory at times when RNO-G stations were active. Blue shaded histogram. Loss of efficiency at large zenith angles attributable to unfavorable Fresnel coefficients for signal refracting into ice. At lower zenith angles, incident signal is increasing horizontally polarized. Maximum solar elevation during summer months at Summit Station is approximately 40 degrees.

Askaryan Radio Array (ARA) experiment[4, 5], these are the only reported coronal mass ejections (CME) reported by the South Polar UHEN experiments.

Unlike RICE, which was parasitically co-deployed in IceCube boreholes, the RNO-G experiment is a dedicated ultra-high energy neutrino observatory[1]. In contrast to ARA¹, RNO-G also includes, as part of its station layout (Figure 2 left), log-periodic dipole array (LPDA) surface antennas designed to both measure down-coming ultra-high energy cosmic rays (UHECR) as well as provide a veto for above-surface noise.

The first observation of solar flares by RNO-G was recorded following the bright Sept. 29, 2022

¹The ARA station design did include 4 surface channels per station, however the data acquisition system for those channels was never adapted to the surface antenna bandwidth

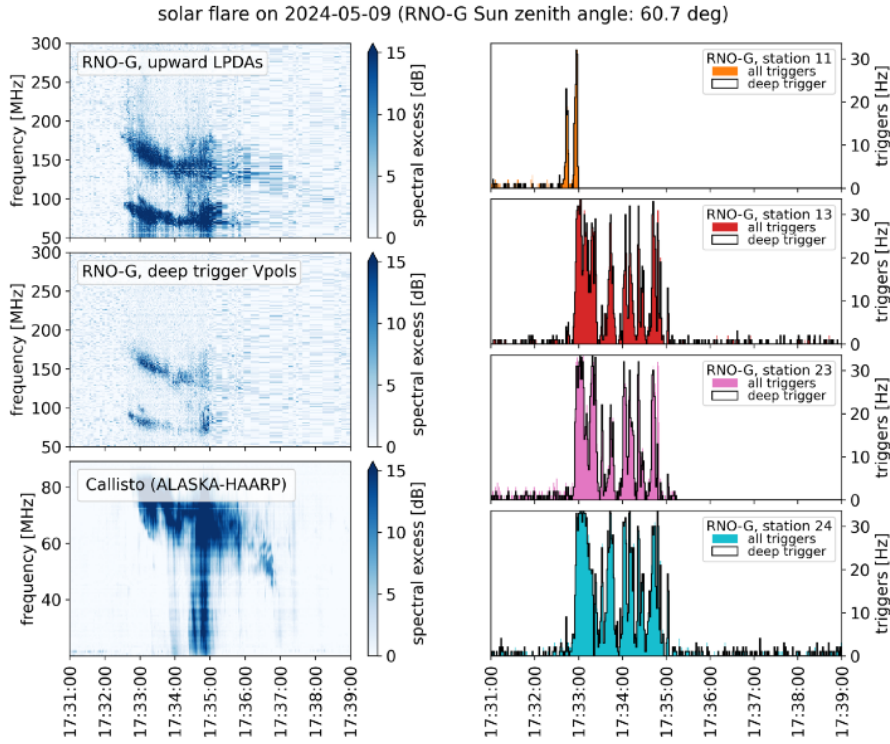


Figure 3: 9May24 solar flare spectrograms (spectral power vs. time) recorded by RNO-G station 11 upward-facing LPDA's (top left), phased-array VPol antennas (middle left), compared with publicly available Callisto network (HAARPS, Alaska, USA) spectrograms. Right column displays time-dependent trigger rates in the four RNO-G stations that triggered surface antennas.

flare; that flare preceded the winter hibernation of the stations as the solar panel output power went sub-critical by only 3 days. Subsequent data analysis indicated that RNO-G's flare trigger efficiency, calculated relative to the dedicated S/WAVES[6] solar observatory is approximately 50%, averaged over all elevation angles (Figure 2 right), prompting a dedicated investigation of solar flare triggers.

The e-Callisto[7] spectrometer network comprises a large number (> 60) of instruments distributed around the world, and allowing continuous (and redundant) monitoring of solar activity, and offers a very useful reference observatory for RNO-G observations. Figure 3 and Figure 4 compare spectrograms for RNO-G receivers with those of the HUMAIN (Belgium) and HAARPS (Alaska) e-Callisto spectrometer (left panels). In the right panels, we see significantly enhanced trigger rates in RNO-G stations, simultaneous with the eCallisto solar flare observations. In contrast to the 2022 solar flare observations, the May, 2024 RNO-G event sample is dominated by surface LPDA triggers. In what follows, we focus primarily on the in-ice VPol RNO-G antenna triggers; 2024 solar flare analysis is currently underway.

Over the duration of the solar flare (in the cases studied here, from 20–180 s), we observe nearly continuous enhancement of RF power over the ambient thermal noise, consistent with a model of prominent emission over $\mathcal{O}(1000 \text{ km})$ length scales, in contrast to impulsive signals generated by neutrinos over meter length scales. Although only $\sim 10\%$ of captured waveforms show distinctive impulses (Figure 5), interferometric reconstruction of the solar source location

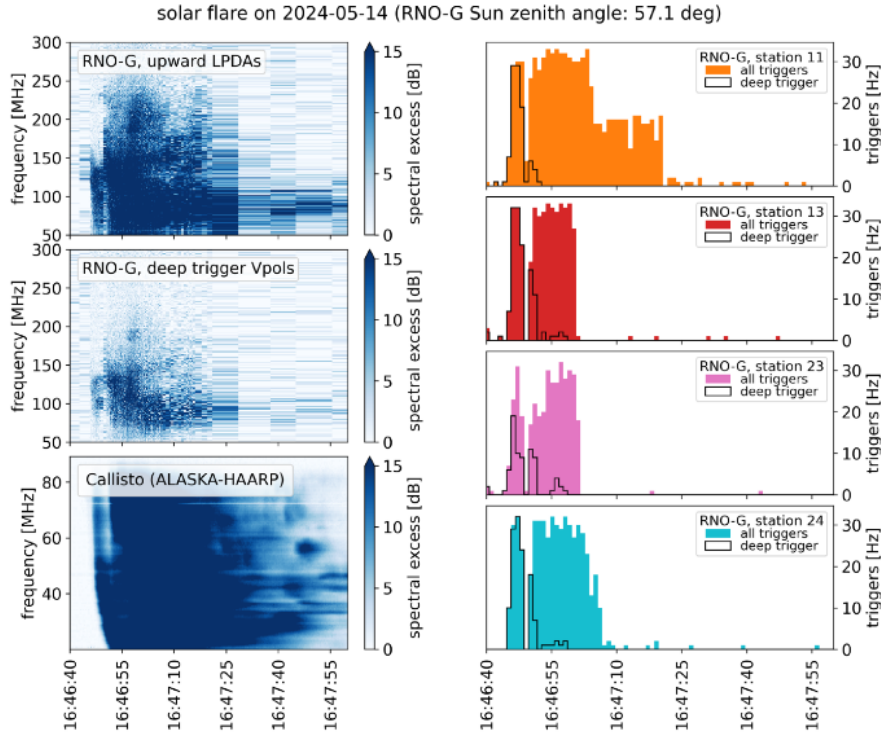


Figure 4: Same as previous figure, for 14May24 solar flare.

is strongly constrained by the fact that the waveforms, albeit somewhat featureless, are strongly correlated in shape, from channel to channel. In the power string display of Figure 5, for example, we observe the clear signature of a down-coming plane wave sweeping through both the VPol (blue) and also HPol (cyan) antennas. Note that the impulse visible in the deeper channels arrives too early in the two uppermost VPol channels ($z=-40$ m and $z=-60$ m) to be visible in the event capture window. Interestingly, the surface LPDA signal response shows only limited deviation from azimuthal symmetry, and not obviously evidencing the expected $\pi/3$ LPDA beamwidth. (Expanding these LPDA beam pattern measurements, as well as the in-ice VPol and HPol gain dependence on elevation, will be a focus of future work.)

Using the channel-to-channel time delays that maximize the overall cross-correlation of the captured waveforms, we can then employ standard interferometry to reconstruct the source azimuth and elevation, using the nuRadioReco[8] software package. The source location in the sky can then be compared with the known solar location and, via a χ^2 minimization procedure, the coordinates of the in-ice antennas that give the best match to the known solar location extracted. This calibration procedure yields typical shifts of 10–15 cm per channel, relative to the initially surveyed antenna locations. The pre- and post-calibration solar reconstructed azimuth and elevation station-by-station are shown in Figure 6; the composite reconstruction is shown in Figure 7; note the elevation compression of the solar image due to refractive effects.

Cross-checks employed to verify the result include: i) dividing the sample into two sub-samples and verifying that the two sub-samples independently yield the same calibration, ii) toggling the

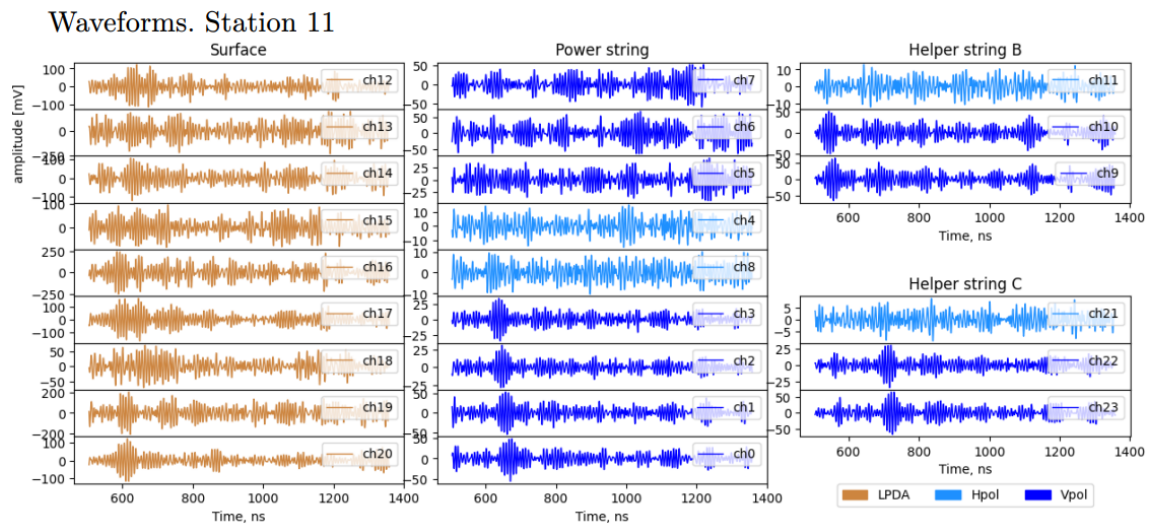


Figure 5: Event waveforms recorded during 14May24 solar flare. Left column (orange) displays 9 surface antenna channels; center column shows (blue) VPol antennas on power string (at depths of -40, -60, -80, -94, -96, -98, -100 m) and (cyan) HPol antennas in center of string. Trigger is formed using bottom VPol antennas. Right column shows signals recorded in ‘Helper Strings’, displaced laterally from Power String by ~ 30 m, including one HPol (cyan) and two VPol (blue) antennas in each borehole.

ice refractive index profile by $\pm 1\%$ and verifying relative stability of the calibrated locations, iii) verifying that lateral shifts are consistent for individual channels on the same string, as expected for antennas deployed in the same borehole.

Summary

"You shake my nerves and you rattle my brain, Too much [science] drives a man insane, You broke my will, but what a thrill, Goodness gracious, great balls of fire."

- J.Z.Lewis, 1957

Over the last two years, the RNO-G detector has triggered on over 100 solar flares. As demonstrated herein, those flares permit precise calibration of antenna locations in-ice[9]. Surface trigger data still to-be-analyzed should permit a similar calibration of the surface LPDA receivers, as well as (given sufficient azimuthal coverage) an *in situ* calculation of the LPDA beam pattern. By contrast, the solar flare sample used by the South Polar experiments is considerably smaller, perhaps owing to the significantly smaller elevation angles attained by the sun. Reconstruction of the ambient sun by interferometry would permit nearly real-time monitoring of antenna response; that effort, albeit unsuccessful thus far, is still in progress.

Acknowledgments

We are thankful to the support staff at Summit Station for making RNO-G possible. We also acknowledge our colleagues from the British Antarctic Survey for building and operating the

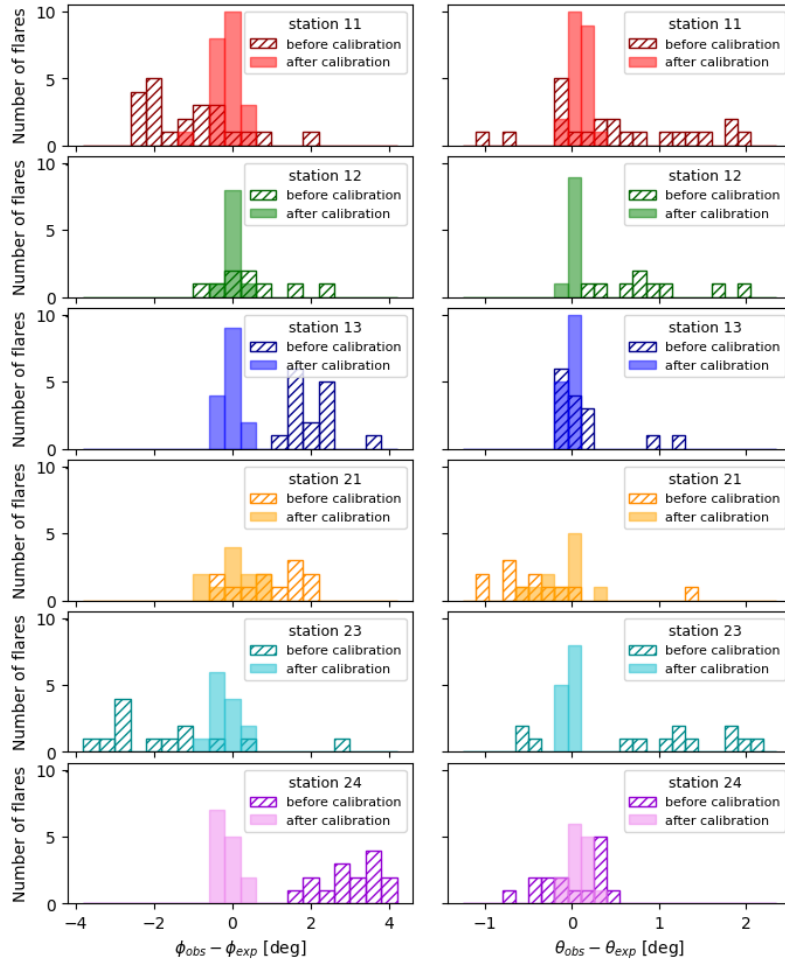


Figure 6: Pre/post-calibration deviations in reconstructed solar azimuth (left) and elevation (right, after accounting for refractive effects) for six stations, using 59 solar flare triggers with highest Signal-to-Noise ratio and waveform impulsivity

BigRAID drill for our project. We would like to acknowledge our home institutions and funding agencies for supporting the RNO-G work; in particular the Belgian Funds for Scientific Research (FRS-FNRS and FWO) and the FWO programme for International Research Infrastructure (IRI), the National Science Foundation (NSF Award IDs 2118315, 2112352, 2111232, 2112352, 2111410, and collaborative awards 2310122 through 2310129), and the IceCube EPSCoR Initiative (Award ID 2019597), the German research foundation (DFG, Grant NE 2031/2-1), the Helmholtz Association (Initiative and Networking Fund, W2/W3 Program), the Swedish Research Council (VR, Grant 2021-05449 and 2021-00158), the Carl Tryggers foundation (Grant CTS 21:1367), the University of Chicago Research Computing Center, and the European Union under the European Unions Horizon 2020 research and innovation programme (grant agreements No 805486), as well as (ERC, Pro-RNO-G No 101115122 and NuRadioOpt No 101116890).

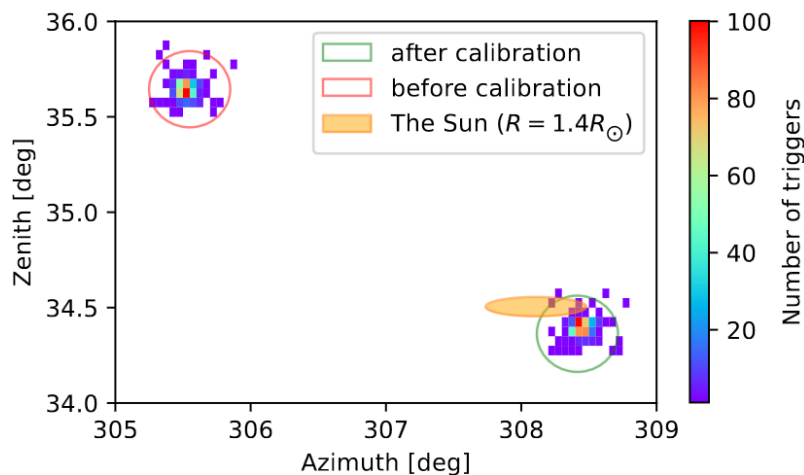


Figure 7: Solar azimuth/elevation reconstruction both prior to, and after calibration. Note the compressed vertical image of the sun due to refractive effects.

References

- [1] Aguilar, Juan A., et al. "Design and sensitivity of the Radio Neutrino Observatory in Greenland (RNO-G)." *Journal of Instrumentation* 16.03 (2021): P03025.
- [2] Carrington, R. C. Description of a singular appearance seen in the Sun on September 1, 1859. *Monthly Notices of the Royal Astronomical Society*, Vol. 20 (1859), p. 13-15, 20, 13-15.
- [3] Kravchenko, I, et al. "Rice limits on the diffuse ultrahigh energy neutrino flux." *Physical Review D—Particles, Fields, Gravitation, and Cosmology* 73.8 (2006): 082002.
- [4] Allison, Patrick, et al. "Design and initial performance of the Askaryan Radio Array prototype EeV neutrino detector at the South Pole." *Astroparticle physics* 35.7 (2012): 457-477.
- [5] Allison, P., et al. "Observation of reconstructable radio emission coincident with an x-class solar flare in the Askaryan radio array prototype station." *arXiv preprint arXiv:1807.03335* (2018).
- [6] Bougeret, Jean-Louis, et al. "S/WAVES: The radio and plasma wave investigation on the STEREO mission." *Space Science Reviews* 136 (2008): 487-528.
- [7] Benz, A. O., et al. "A world-wide net of solar radio spectrometers: e-CALLISTO." *Earth, Moon, and Planets* 104 (2009): 277-285.
- [8] Glaser, Christian, et al. "NuRadioMC: Simulating the radio emission of neutrinos from interaction to detector." *The European Physical Journal C* 80 (2020): 1-35.
- [9] Agarwal, S., et al. "Solar flare observations with the Radio Neutrino Observatory Greenland (RNO-G)." *arXiv preprint arXiv:2404.14995* (2024), and accepted for publication in *Astroparticle Physics*.